Geometric symmetry of the solar surface of hooves of Thoroughbred racehorses

Elizabeth Roland, MS; Susan M. Stover, DVM, PhD; Maury L. Hull, PhD; Katie Dorsch

Objective—To define a 3-dimensional (3-D) coordinate system with clear definitions of origins and axes relative to hoof anatomic features and determine whether solar surfaces of Thoroughbred racehorse hooves have geometric asymmetry in the mediolateral and dorsopalmar directions.

Sample Population—Left forelimb hooves from 20 Thoroughbred racehorse cadavers.

Procedure—A right-handed 3-D coordinate axes system centered on the collateral sulci was defined for the left front hoof. Orthogonal distances of anatomic features from the dorsopalmar axis and the plane coincident with the ground were measured and compared between medial and lateral sides and between dorsal and palmar regions of the hoof.

Results—The hoof was wider and had a greater radius laterally than medially. The most distal part of the lateral bar of the frog was further from the dorsopalmar axis than that of the medial bar. Overall, mediolateral asymmetries in depth were not observed. The sole at the perimeter was deeper medially in the dorsal part of the hoof and laterally in the palmar part, with depth overall being greater palmarly than dorsally. Most features had dorsopalmar asymmetry.

Conclusions and Clinical Relevance—When the angle bisected by the collateral sulci is used to determine the dorsopalmar axis of the hoof, most central structures (bars and collateral sulci) have mediolateral symmetry. However, the hoof wall and sole have some mediolateral asymmetries and most structures have dorsopalmar asymmetry. These findings may assist the development of devices for attachment to hooves and studies of the interaction of hooves with bearing surfaces. (*Am J Vet Res* 2003;64:1030–1039)

The hoof capsule is the interface between the horse and ground that is subject to trauma and injuries during locomotion; it is composed of several structures including the hoof wall, sole, and frog. These structures have unique shapes and are made of tissues with different compliances[1-5] that result in different biomechanical functions during weight bearing and locomotion. At rest on a hard surface, the hoof wall transfers most of the load to the limb.[6,7] With either greater loads or a more conforming surface, the ground contact area may increase, additional hoof structures may contact the surface, or the hoof capsule may deform so that structures may abnormally share in load transfer, which potentially causes damage.[6-9]

The collection of quantitative data regarding the structures of the solar surface of the hoof capsule would enhance the understanding of morphologic features of the foot and load transfer between the ground surface and hoof structures.[10] Furthermore, this information would enable therapeutic horseshoes to be designed more precisely to redirect pressure away from damaged tissues to other structures of the hoof.[11] Improvements in horseshoe design would likely enhance injury prevention as well.[12]

To characterize and compare the structures on the solar surface of the hoof, a coordinate system is necessary. Two-dimensional locations of solar structures are ambiguous without reference to a coordinate system. Although the mediolateral symmetry of the hoof has been described,[10] the location of the axis of symmetry was not stated, which makes direct comparisons of those data with findings of other studies impossible. Development of a coordinate system would provide a reference for morphologic evaluation of structures of the solar surface of the hoof and for tracking the center of pressure for ground contact forces during motion. Information regarding the center of pressure obtained in studies[13-16] has been difficult to interpret, because key reference points were not clearly defined. Because development of a coordinate system would allow comparison of structures within a hoof and among hooves used in different studies, the purpose of the study reported here was to define a **3-dimensional (3-D)** coordinate system with clear definitions of the origin and axes relative to prominent hoof anatomic characteristics or features and confirm the reproducibility of this system. In addition, the coordinate system was used to collect data from a sample of Thoroughbred racehorse hooves to characterize structures on the solar surface. Furthermore, because physical attributes of the hoof, including mediolateral symmetry, are possible indicators of risk for injury and unsoundness,[10,17] this study was intended to examine mediolateral and dorsopalmar variations in central and peripheral solar structures (in ground surface plane and depth).

Materials and Methods

Specimens—Feet from left cadaveric forelimbs of 20 Thoroughbred racehorses that had been in active racing or race training were studied; these horses were between 2 and 6 years of age (mean ± SD, 3.5 ± 1.3 years; age of 1 horse not known), and there were 8 females and 12 males (including 9

Recieved September 27, 2002.
Accepted February 12, 2003.
From the Biomedical Engineering Program (Roland, Stover, Hull); and the J. D. Wheat Veterinary Orthopedic Research Laboratory (Stover, Dorsch), Department of Anatomy, Physiology, and Cell Biology, School of Veterinary Medicine, University of California, Davis, CA 95616. Elizabeth (Roland) Barrows' current address is 2036 Sloop Point Loop Rd, #8A, Hampstead, NC 28443.
Supported by a grant from the Grayson-Jockey Club Research Foundation Incorporated.
Address correspondence to Dr. Stover.

neutered males). Hooves were collected through the California Horse Racing Board Postmortem Program conducted by the California Animal Health and Food Safety Laboratory System. Reasons for euthanasia included bone fracture in 14 horses (proximal sesamoid bone fracture [n = 6], metacarpal fracture [3], carpal fracture [2], humeral fracture [2], and pastern fracture [1]) and nonmusculoskeletal disorders in 6 horses. Horseshoes were removed from the hooves. Hooves were not trimmed or frozen and were measured the same day that they were received from the diagnostic laboratory (always within 3 days of euthanasia of the horse). Hooves that were fitted with corrective or rolled-toe shoes, had loss of hoof wall from the dorsal aspect at the solar surface, or had hoof wall defects were excluded from the study.

Coordinate system—The 3-D coordinate system was fixed to the left front hoof on the basis of reliable anatomic features (**Fig 1**). The x-y plane was coincident with the flat plane ground surface of the hoof. The x-axis was a line that bisected the angle formed by visual estimation of best-fit straight lines in the deep collateral sulci (the most proximal part of the collateral sulci) adjacent to the frog. The origin of the x-axis was the midpoint of the line extending between the intersection of the axis with a perpendicular line through the most dorsal point on the hoof wall and the intersection of the axis with a line drawn between the most palmar portions of the medial and lateral angles of the wall at the ground contact level. The positive direction of the x-axis was dorsal to the origin. The y-axis was perpendicular to the x-axis through the origin; the positive direction of the y-axis was lateral on the left hoof. The z-axis, normal to the x-y plane (positive direction proximal to the x-y plane) completed the right-handed coordinate system. A right-handed coordinate system is illustrated by rotating the x-axis onto the y-axis with the fingers of the right hand while the thumb is pointed outwards in the plane of the hand. The direction in which the thumb points defines the positive direction of the z-axis.

A cylindrical coordinate system centered on the z-axis was used for measurements of the perimeter of the hoof (Fig 1). The angular measurement had its reference at the positive x-axis and increased in value toward the positive y-axis.

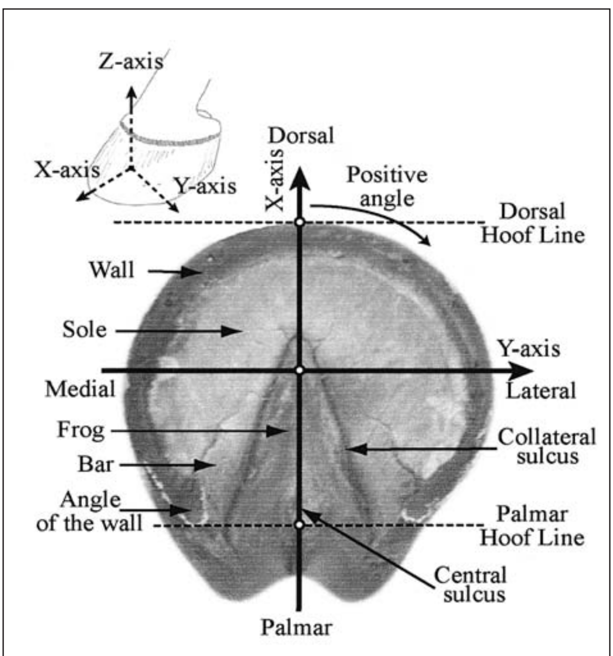

Figure 1—Illustration of the application of the 3-dimensional and cylindrical coordinate systems to the hoof of a Thoroughbred racehorse by use of anatomic features of the solar surface of the hoof. Orientation of the x, y, and z axes is relative to the left front hoof (upper left). The x-axis bisects the angle formed by the deep collateral sulci (dashed lines) adjacent to the frog. The origin of the x-axis is halfway between the dorsal hoof line and the palmar hoof line. White chalk was used to outline the palmar aspect of the bearing surface of the hoof wall at the heels. The reference of the cylindrical coordinate system begins at the positive portion of the x-axis and increases in value toward the positive portion of the y-axis (Underlying hoof image courtesy of Albert J. Kane).

Reproducibility of axis placement—The assistance of 7 people (including medical, veterinary, and biomedical engineering graduate students and faculty) was obtained to test the reproducibility of coordinate axis placement on the hoof. A high definition color photograph of 1 of the hooves included in our study was placed under a transparent film. The film was marked for alignment with the photograph. Each person was given a copy of the section of this article in which the method for locating the x-axis and the origin was described, as well as definitions of some of the hoof-specific terms, and asked to locate the x-axis and the origin by means of any tools necessary. Error for all experimental axes and origins was calculated as the difference between the location of the experimental axes and origins and that of a standard axis and origin placed by 1 of the study investigators (ER). The comparison entailed computing both the accuracy (mean error) and precision (SD of the error) of the x and y coordinates of the origin and the accuracy and precision in the angle of rotation of the x-axis.

Definitions of lines and locations based on landmarks that were used for quantification of the structures evident on the solar surface of the hoof—Landmarks (aspects of the solar surface of the hoof that were used for orientation) included features (such as points, borders, and surfaces) of the hoof wall, frog, central sulcus, collateral sulci, and bars of the hoof wall structures (Fig 1). Lines were straight or curved marks (real or imaginary) that represented a boundary, division, or contour (including the contours between structures on the solar surface of the hoof, contours describing features of the structures on the solar surface of the hoof, and straight lines marking divisions on the solar surface of the hoof). Locations were defined as any point distinguished by either the intersection of 2 lines or as a definitive landmark on a structure on the solar surface of the hoof.

Lines and locations were defined relative to landmarks (Fig 1, **2 and 3**). The dorsal hoof line was a line parallel to the y-axis that crossed the x-axis at the most dorsal aspect of the hoof wall at the solar surface. The palmar hoof line was a line parallel to the y-axis that crossed the x-axis at the intersection of a line drawn between the caudal aspect of the angles of the wall and the x-axis. The palmar foot location was the intersection of a straight line drawn between the palmar points on the bulbs of the heel and the x-axis. The widest hoof locations were the lateral and medial locations of the widest part of the hoof along a single straight line that was perpendicular to the x-axis. The apex of the frog was the location at the dorsal aspect of the frog. The distal frog lines were lines on the lateral and medial bars of the frog that corresponded to the contour lines along the intersection of the distal surface of the frog and the abaxial surface of the frog for each bar. The deep collateral sulci lines were contour lines that traced the proximal portion of each collateral sulcus. The dorsal central sulcus location was the dorsal point of the central sulcus, and the palmar central sulcus location was the palmar point of the central sulcus. The edge of central sulcus lines were the lateral and medial contour lines located where the slope of the dis-

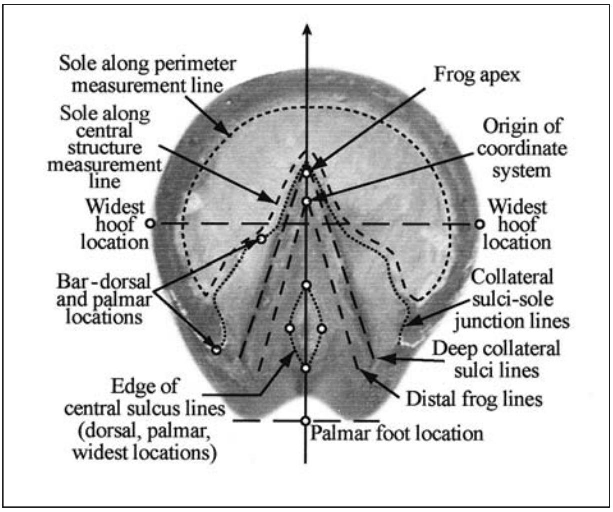

Figure 2—Illustration of the solar surface of the left front hoof of a Thoroughbred racehorse demonstrating lines and their relationships to landmarks.

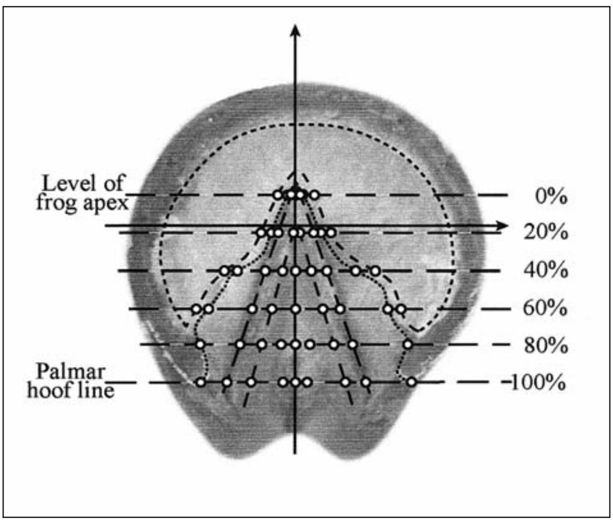

Figure 3—Illustration of the solar surface of the left front hoof of a Thoroughbred racehorse demonstrating locations and their relationships to measurement lines.

tal surface of the frog changed to the steeper slope of the central sulcus. The widest central sulcus locations were medial and lateral locations of the widest part of the central sulcus at the intersections of a single straight line perpendicular to the x-axis with the medial and lateral edge of central sulcus lines. Central sulcus measurement lines were 4 equally spaced straight lines (at 0, 33, 67, and 100% positions along the dorsopalmar orientation) that were perpendicular to the x-axis beginning at the dorsal and ending at the palmar central sulcus locations. Central sulcus measurement locations were the intersections of central sulcus measurement lines with the edge of central sulcus lines. Collateral sulci-sole junction lines were medial and lateral contour lines indicating where the steep slope of the collateral sulcus leveled out to become the sole. Palmarly, this was contiguous with the axial edge of the bar of the hoof wall. Frog and collateral sulci measurement lines were 6 equally spaced straight lines (at 0, 20, 40, 60, 80, and 100% positions along the dorsopalmar orientation) that were perpendicular to the x-axis beginning at the apex of the frog and ending at the palmar hoof line. Frog and collateral sulci measurement locations were points of intersection of the frog and collateral sulci measurement lines with the distal frog lines, the deep collateral sulci lines, and the collateral sulci-sole junction lines. Bar locations were the dorsal and palmar locations of the bars of the hoof wall (located by means of the cylindrical coordinate system and translated to x-y coordinates). Sole along the perimeter measurement line was an imaginary line on the sole of the hoof approximately 0.5 cm inside of the hoof wall; this line is axial to the white line on the sole and was used only for measurement of depth parameters. The sole along the central structure measurement lines were imaginary lines on the sole of the hoof approximately 0.5 cm abaxial to the respective collateral sulci-sole junction lines; these lines were used only for measurement of depth parameters.

Definitions of parameters—Parameters were distances measured to describe the shape and size of structures on the solar surface of the hoof (**Fig 4**). Overall hoof parameters included the ground surface length (distance along the x-axis between the dorsal hoof line and the palmar hoof line), total foot length (distance along the x-axis between the dorsal hoof line and the palmar foot location), and hoof width (distance between the widest hoof locations). Frog parameters included frog length (distance between the apex of the frog and the intersection of the palmar hoof line with the x-axis), distal frog widths (distances between the lateral and medial distal frog lines along the frog and collateral sulci measurement lines), and proximal frog widths (distances between the lateral and medial deep collateral sulci lines along the frog and collateral sulci measurement lines). Central sulcus parameters included central sulcus length (distance between the dorsal central sulcus location and palmar central sulcus location [parallel to the x-axis]), central sulcus widths (distances between the medial and lateral edge of central sulcus lines along the central sulcus measurement lines), and widest part of the central sulcus (distance, perpendicular to the x-axis, between the widest central sulcus locations). Collateral sulci parameters included collateral sulci widths (distances between either the lateral or medial collateral sulcus-sole junction line and the ipsilateral distal frog line along the frog and collateral sulci measurement lines) and bar length (distance between the dorsal and palmar locations on the bars of the hoof). Perimeter parameters included measurements of hoof wall radii (distances from the origin to the abaxial edge of the wall at 15° increments [at corresponding medial and lateral radial positions determined by means of the cylindrical coordinate system: at 345°, 15°; 330°, 30°; and so forth to 195°, 165°]) and wall thicknesses (radial thicknesses of the firm horn tissue associated with the wall at the solar surface taken at 15° increments [at corresponding medial and lateral radial positions determined by means of the cylindrical coordinate system: at 345°, 15°; 330°, 30°; and so forth to 225°, 135°]).

Depth parameters measured along the direction of the z-axis from the x-y ground surface plane at locations related to the frog and collateral sulci measurement lines (**Fig 5**), included midline depths (depths to the solar surface directly along the x-axis at intersections with the frog and collateral sulci measurement lines), central sulcus depths (depths of the edge of central sulcus lines when present at the intersection of the frog and collateral sulci measurement lines), frog depths (depths to the frog at the intersections between the distal frog lines and the frog and collateral sulci measurement lines), deep collateral sulci depths (depths to the proximal locations of the collateral sulci at the intersections between the deep collateral sulci lines and frog and collateral sulci measurement lines), collateral sulci edge depths (depths to the collateral sulci-sole junction lines, including the bars of the hoof wall, at the intersections between these lines and the frog and collateral sulci measurement lines), sole depths at central structure measurement line (depths to the sole at the intersections of the sole at central structure measurement

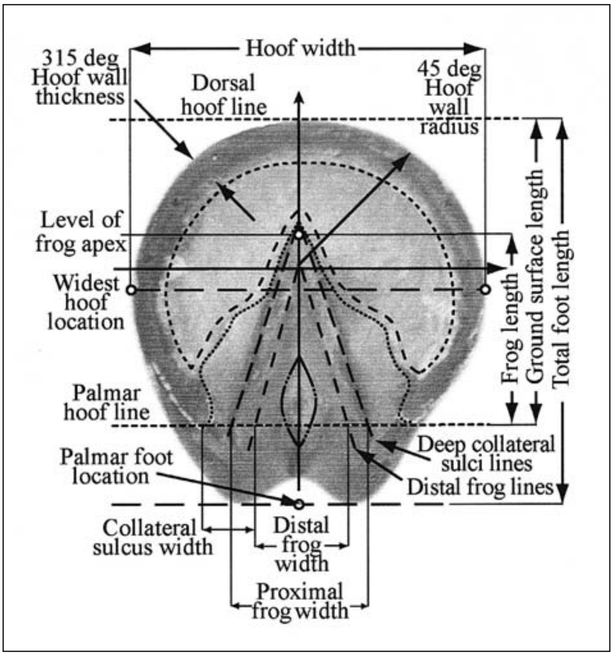

Figure 4—Illustration of the solar surface of the left front hoof of a Thoroughbred racehorse demonstrating distance measurements.

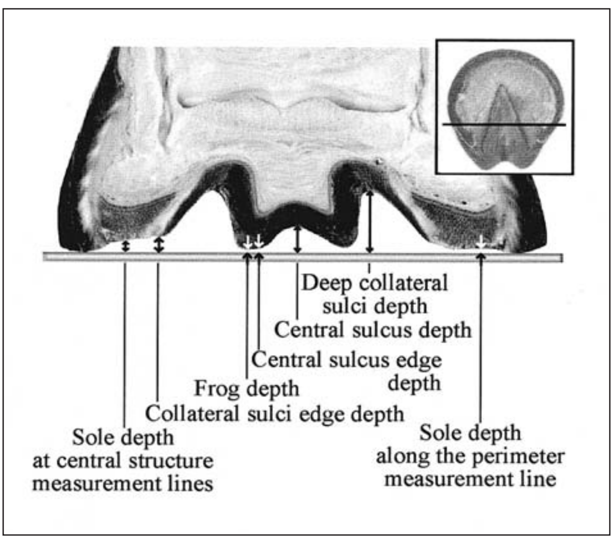

Figure 5—Illustration of dorsal section of the left front hoof of a Thoroughbred racehorse demonstrating depth measurements. Orientation for the level of the dorsal section is indicated in the upper right inset.

lines with the frog and collateral sulci measurement lines), and sole along the perimeter measurement line depths (depths to the sole at the intersections of the sole along the perimeter measurement line and radial lines at 15º intervals [at corresponding medial and lateral radial positions by means of the cylindrical coordinate system: at 345º, 15º; 330º, 30º; and so forth to 225º, 135º]).

Tools—Measurements were made with a 6- or 8-inch caliper set with a digital display (capable of measurement to an accuracy of 0.01 mm), a pair of rectangular acrylic plates, and a protractor. Cross-sectional dimensions of the rectangular tip of the caliper used for the depth measurements were 2.1 X 1.5 mm. Two custom-made, clear acrylic plates with 4.8-mm-wide linear slots were used to mark lines that were required for repeated measurements (eg, frog and collateral sulci measurement lines) and locate radial measurement locations, and functioned as a level base for the depth measurements. One plate contained a single slot aligned parallel to 1 side of the plate. With the long axis of the slot aligned perpendicular to the x-axis, this plate was used to apply both the line defining the y-axis and measurement lines parallel to this axis. This plate was also used to ensure that depth measurements among the central structures of the hoof were perpendicular to the plane of the template. Perpendicularity was achieved by measurement of depths though the slot with the caliper squared against the plate. The other plate had radially oriented slots positioned every 15º, was used for all of the measurements made at 15º intervals around the hoof, and ensured that depth measurements were perpendicular to the plane of the template. A transparent plastic protractor was used to measure the dorsal and palmar angular locations of the bars of the wall in the cylindrical coordinate system, because the bars rarely coincided with the 15º radial slots in the plate. Radial data were then converted to the Cartesian coordinate system for analysis.

Table 1—General characteristics of hooves from the left forelimbs of 20 Thoroughbred racehorse cadavers

Variable	Location	Mean ± SD (mm)
Overall hoof parameters		
	Ground surface length	115.60 ± 6.25
	Total foot length	145.02 ± 6.35
	Hoof width	122.03 ± 6.52
Frog parameters		
	Frog length	70.44 ± 6.44
	Distal frog widths	
	0%	1.73 ± 1.49
	20%	5.31 ± 3.14
	40%	9.70 ± 3.99
	60%	16.75 ± 4.49
	80%	25.97 ± 5.08
	100%	34.30 ± 8.14
	Proximal frog widths	
	0%	4.81 ± 2.35
	20%	17.14 ± 3.20
	40%	25.80 ± 4.17
	60%	33.21 ± 4.12
	80%	41.08 ± 4.36
	100%	46.70 ± 7.55
Central sulcus parameters		
	Central sulcus length	46.09 ± 6.41
	Central sulcus width	
	0%	0.68 ± 1.04
	33%	15.84 ± 2.90
	67%	19.97 ± 5.41
	100%	1.31 ± 1.72
	Widest part of the central sulcus	21.93 ± 3.86
Depth parameters		
	Midline depths	
	0%	6.39 ± 2.52
	20%	4.72 ± 2.11
	40%	3.07 ± 1.92
	60%	3.79 ± 1.47
	80%	7.71 ± 2.66
	100%	9.61 ± 3.46

Statistical analyses—All statistical analyses were performed by use of commercial statistical software.[a] The mean and SD values were calculated for centrally located structures. Data for all locations and parameters were tested for normality with a Kolmogorov-Smirnov test. Because the data were normally distributed for > 90% of the locations and parameters, data were analyzed by means of parametric tests. For solar structures that could be compared, a repeated measures ANOVA was used to assess mediolateral side and dorsopalmar

Table 2—Mediolateral comparison of location distances (mean ± SD) from the dorsopalmar axis in the ground surface plane of hooves from the left forelimbs of 20 Thoroughbred racehorse cadavers

Location	Position	N	Measurements: Medial (mm)	Measurements: Lateral (mm)	*P* values from repeated measures ANOVA and post-hoc comparisons: Side (medial vs lateral)	Position (dorsal vs palmar)	Side × position interaction
Widest hoof locations		20	60.1 ± 3.8	61.9 ± 2.9	< 0.001	na	na
Distal frog lines					0.03*	< 0.001*	0.22*
	0%	19	0.9 ± 0.9	1.0 ± 0.7	0.83	a	na
	20%	20	2.5 ± 2.0	2.7 ± 1.6	0.38	b	na
	40%	20	4.7 ± 2.0	5.0 ± 2.2	0.22	c	na
	60%	20	8.1 ± 2.2	8.7 ± 2.5	0.07	d	na
	80%	20	12.4 ± 2.5	13.5 ± 2.8	0.005	e	na
	100%	19	16.8 ± 3.9	17.8 ± 4.9	0.34	f	na
Deep collateral sulci lines					0.60*	< 0.001*	0.99*
	0%	19	2.6 ± 1.3	2.3 ± 1.1	na	a	na
	20%	20	8.8 ± 1.8	8.3 ± 1.5	na	b	na
	40%	20	13.1 ± 2.2	12.7 ± 2.2	na	c	na
	60%	20	16.8 ± 2.4	16.4 ± 2.0	na	d	na
	80%	20	20.4 ± 2.4	20.6 ± 2.1	na	e	na
	100%	20	22.9 ± 4.6	23.8 ± 3.3	na	f	na
Collateral sulci-sole junction lines					0.46*	< 0.001*	0.003*
	0%	20	6.7 ± 2.0	6.6 ± 2.3	na	a	‡
	20%	20	14.5 ± 2.8	13.8 ± 2.7	na	b	‡
	40%	20	21.9 ± 4.4	21.4 ± 4.1	na	c	‡
	60%	20	28.9 ± 5.1	30.1 ± 4.9	na	d	‡
	80%	20	31.4 ± 4.6	32.4 ± 4.7	na	e	‡
	100%	20	28.3 ± 4.8	28.6 ± 5.2	na	d	‡
Widest central sulcus locations		20	10.9 ± 2.6	10.7 ± 2.1	0.83	na	na
Edge of central sulci lines					0.74*	< 0.001*	0.06*
	0%	20	0.1 ± 0.9	0.7 ± 0.9	na	a	na
	33%	20	7.9 ± 1.6	8.0 ± 1.6	na	b	na
	67%	20	10.2 ± 3.0	9.5 ± 3.0	na	c	na
	100%	20	0.7 ± 1.4	0.4 ± 1.1	na	a	na

*Values from the repeated measures ANOVA; other values are from paired *t* tests. Levels of position with the same lowercase letter are not significantly different from each other (post-hoc pairwise contrasts). ‡Described in the text.
N = Number of hooves from which measurements were obtained. na = Not available.

position differences in medial and lateral locations, parameters, and depths. The effects of side (medial or lateral), position (dorsal to palmar), and the 2-way interaction between side and position (side × position) were included as fixed effect independent variables. Post-hoc paired *t* tests were performed when the side main effect was significant (to investigate the side effect in greater detail). Post-hoc pairwise contrast comparisons were performed when either the position main effect or the interaction was significant. When the position main effect and side × position interaction were both significant, pairwise contrast comparisons were still performed on the position main effect, because the position effect was always large in comparison to the interaction effect. All pairwise contrast comparisons were performed on quantities computed by pooling the data on both the medial and lateral sides. Significance was set at $P \leq 0.05$ and a trend at $0.05 < P < 0.10$.

Results

From the reproducibility portion of the study, the accuracy of the x-coordinate of the origin was 0.0 mm, and that of the y-coordinate was –0.4 mm with a precision of 0.6 and 0.8 mm, respectively. Additionally, the accuracy of the rotation of the x-axis about the *z*-axis was –0.22° with a precision of 0.28°.

From data regarding the overall characteristics of the solar surface of the hoof, the mean ground surface length was less than the mean width (**Table 1**). Distal and proximal frog width parameters increased in magnitude from dorsal to palmar. In contrast, the central sulcus widths were narrowest at the dorsal and palmar positions and widest in the center of the structure. Midline depth was greatest at the extremes of the frog length.

Differences in the medial and lateral locations were evident for a number of features, and dorsopalmar relationships were apparent for all features (**Table 2**). The lateral aspect of the hoof was wider than the medial aspect by 1.8 mm ($P < 0.001$). The distances from the midline to the distal frog lines were greater for the lateral bar of the frog than they were for the medial bar ($P = 0.03$); distances increased from dorsal to palmar ($P < 0.001$). Medial and lateral aspects of the deep collateral sulci were not significantly ($P = 0.60$) different. Collateral sulci-sole junction lines were further from the x-axis palmarly than dorsally ($P < 0.001$). Additionally, a significant ($P = 0.003$) interaction was evident where the collateral sulci-sole junction lines were further from the x-axis to the medial side in the dorsal half of the hoof (0 to 40%) and from the x-axis to the lateral side on the palmar half of the hoof (60 to 100%). In contrast to data regarding the

Table 3—Mediolateral comparison of parameter magnitudes in the ground surface plane (mean ± SD) of hooves from the left forelimbs of 20 Thoroughbred racehorse cadavers

			Measurements		*P* values from repeated measures ANOVA and post-hoc comparisons		
Location	**Position**	**N**	**Medial (mm)**	**Lateral (mm)**	**Side (medial vs lateral)**	**Position (dorsal vs palmar)**	**Side X position interaction**
Hoof radii					0.008*	< 0.001*	0.70*
	360° (0°)	20	57.8 ± 3.0		na	a	na
	345°, 15°	20	57.9 ± 3.3	58.0 ± 3.4	0.93	a	na
	330°, 30°	20	57.7 ± 3.2	58.0 ± 3.2	0.52	a	na
	315°, 45°	20	57.2 ± 3.2	58.2 ± 3.2	0.06	a	na
	300°, 60°	16	56.9 ± 3.2	58.8 ± 2.8	0.003	a	na
	285°, 75°	18	57.2 ± 3.3	59.7 ± 2.5	0.005	a	na
	270°, 90°	17	59.8 ± 3.3	61.2 ± 2.9	0.009	a,b	na
	255°, 105°	18	61.9 ± 3.9	63.3 ± 2.8	0.02	b,c	na
	240°, 120°	19	63.6 ± 4.1	65.0 ± 3.2	0.005	c,d	na
	225°, 135°	20	65.2 ± 4.0	66.2 ± 3.7	0.02	d,e	na
	210°, 150°	20	66.5 ± 4.0	67.1 ± 4.9	0.28	d,e	na
	195°, 165°	20	66.7 ± 4.1	67.4 ± 4.2	0.03	e	na
Wall thicknesses					0.90*	0.01*	0.91*
	360° (0°)	20	6.1 ± 1.0		na	a,b,c	na
	345°, 15°	20	6.0 ± 1.2	5.9 ± 1.1	na	b,c	na
	330°, 30°	20	6.5 ± 0.9	6.3 ± 1.1	na	a,b,c	na
	315°, 45°	19	7.0 ± 1.2	6.7 ± 1.1	na	a	na
	300°, 60°	15	6.7 ± 1.1	6.5 ± 1.1	na	a,b,c	na
	285°, 75°	18	6.6 ± 1.1	6.7 ± 1.1	na	a,b	na
	270°, 90°	15	6.8 ± 0.9	6.6 ± 0.9	na	a,b	na
	255°, 105°	15	6.3 ± 0.9	6.2 ± 0.9	na	a,b,c	na
	240°, 120°	18	5.9 ± 0.8	5.9 ± 1.0	na	c	na
	225°, 135°	16	6.5 ± 1.0	6.3 ± 1.3	na	a,b,c	na
Collateral sulci widths					0.09*	< 0.001*	0.03*
	0%	20	5.9 ± 2.3	5.6 ± 2.3	na	a	‡
	20%	20	11.9 ± 3.0	11.1 ± 3.2	na	b	‡
	40%	20	17.7 ± 4.8	16.4 ± 3.9	na	c	‡
	60%	20	20.8 ± 4.6	21.4 ± 5.3	na	d	‡
	80%	20	19.0 ± 4.7	18.9 ± 4.7	na	e	‡
	100%	19	11.3 ± 4.8	10.8 ± 5.0	na	b	‡
Bar length		20	43.4 ± 6.1	42.0 ± 7.8	na	na	na

*Values from the repeated measures ANOVA; other values are from paired *t* tests. Levels of position with the same lowercase letter are not significantly different from one another (post-hoc pairwise contrasts).
‡Described in the text.
N = Number of hooves from which measurements were obtained. na = Not available.

collateral sulci-sole junction lines, edge of central sulcus lines in the middle of the range (ie, 33 and 67%) were further from the x-axis than at the extremes of the range (ie, 0 and 100%; $P < 0.001$). Moreover, there was a trend for the edge of the central sulcus to be wider laterally on the dorsal half of the hoof but wider medially on the palmar half of the hoof ($P = 0.06$).

Only 1 set of parameters that described a structure measured in the ground surface plane varied significantly mediolaterally, whereas all parameters showed significant dorsopalmar variance (**Table 3**). Hoof radii parameters were larger laterally than medially in all comparable positions measured ($P = 0.008$) and also larger dorsally than palmarly ($P < 0.001$) except on the medial side between 285 and 330°. Wall thickness did not vary significantly mediolaterally ($P = 0.90$) but was widest between the toe and quarters and thinnest between the quarters and the angles of the heel ($P = 0.01$). Collateral sulcus widths were largest near the middle of the sulcus ($P < 0.001$), with a significant interaction evident where the medial side was wider at 40% and the lateral side was wider at 60% ($P = 0.03$). Medial and lateral bar lengths were not different ($P = 0.19$).

All depth parameters differed ($P \leq 0.02$) from dorsal to palmar aspects, but none of the depths differed between medial and lateral sides ($P \geq 0.19$; **Table 4**). Depth of the central sulcus was greater palmarly than dorsally ($P = 0.02$). Depth of the distal frog line was greater ($P < 0.001$) toward the apex of the frog (dorsally) than palmarly. The deep collateral sulci lines had the least depth at the dorsal and palmar extremes ($P < 0.001$). The depth of the collateral sulci edges was greater dorsally than palmarly ($P < 0.001$). A significant ($P < 0.05$) interaction was evident in that the lateral value at the 60% level was higher than the medial value, compared with the 0, 20, 40, and 100% levels at which the medial values were higher than the lateral values. The depth of the sole at the central structure was greater ($P < 0.001$) dorsally than palmarly, and a significant interaction was evident in that the difference between lateral and medial values at the 40% level was higher than the values at the other levels ($P = 0.02$). The sole at the perimeter measurement line depths were greater ($P < 0.001$) palmarly than dorsally except at the toe where the depth was larger than depths near the toe. A significant interaction was evi-

Table 4—Mediolateral comparison of depth parameters (mean ± SD) of hooves from the left forelimb of 20 Thoroughbred racehorse cadavers

			Measurements		*P* values from repeated measures ANOVA and post-hoc comparisons		
Location	**Position**	**N**	**Medial (mm)**	**Lateral (mm)**	**Side (medial vs lateral)**	**Position (dorsal vs palmar)**	**Side X position interaction**
Central sulcus					0.23*	0.02*	0.27*
	60%	18	3.0 ± 1.8	2.6 ± 1.8	na	a	na
	80%	20	3.0 ± 2.2	2.6 ± 2.0	na	a,b	na
	100%	18	3.4 ± 2.0	3.7 ± 2.4	na	b	na
Distal frog					0.42*	< 0.001*	0.87*
	0%	18	6.5 ± 2.4	6.6 ± 2.7	na	a	na
	20%	20	5.3 ± 2.6	5.4 ± 2.3	na	b	na
	40%	20	3.8 ± 2.4	3.8 ± 2.5	na	c	na
	60%	20	3.5 ± 2.2	3.4 ± 2.3	na	c	na
	80%	20	3.5 ± 2.7	3.8 ± 2.9	na	c	na
	100%	20	3.5 ± 2.8	3.8 ± 2.5	na	c	na
Deep collateral sulci lines					0.60*	< 0.001*	0.99*
	0%	20	10.4 ± 2.6	10.3 ± 2.8	na	a	na
	20%	20	12.8 ± 2.5	12.4 ± 2.4	na	b	na
	40%	20	13.4 ± 2.7	13.3 ± 3.0	na	c	na
	60%	20	14.9 ± 3.8	14.8 ± 4.2	na	d	na
	80%	20	16.6 ± 2.9	16.2 ± 3.2	na	e	na
	100%	19	11.6 ± 4.6	11.2 ± 4.6	na	a,b,c	na
Collateral sulci edges					0.62*	< 0.001*	0.03*
	0%	20	8.1 ± 2.1	7.8 ± 1.8	na	a	‡
	20%	20	8.6 ± 1.6	8.1 ± 1.7	na	a	‡
	40%	20	6.9 ± 1.9	6.8 ± 2.1	na	b	‡
	60%	20	4.3 ± 1.9	4.9 ± 2.4	na	c	‡
	80%	20	1.6 ± 0.8	1.7 ± 1.1	na	d	‡
	100%	20	3.4 ± 1.9	3.2 ± 2.0	na	e	‡
Sole at central structure					0.19*	< 0.001*	0.02*
	0%	20	7.0 ± 1.7	7.2 ± 1.6	na	a	‡
	20%	20	7.4 ± 1.4	7.7 ± 1.3	na	b	‡
	40%	19	5.3 ± 1.8	6.1 ± 2.0	na	c	‡
	60%	20	2.8 ± 1.4	3.0 ± 2.0	na	d	‡
Sole at perimeter					0.41*	< 0.001*	0.05*
	360° (0°)	20	1.8 ± 0.9		na	a,b	na
	345°, 15°	20	1.5 ± 0.6	1.4 ± 0.8	na	a	‡
	330°, 30°	20	1.6 ± 0.6	1.6 ± 0.7	na	a	‡
	315°, 45°	20	1.8 ± 0.8	1.7 ± 0.9	na	a	‡
	300°, 60°	20	2.1 ± 0.8	2.3 ± 1.3	na	b	‡
	285°, 75°	20	2.2 ± 0.9	2.7 ± 1.2	na	c	‡
	270°, 90°	19	2.4 ± 0.6	2.7 ± 1.3	na	c	‡
	255°, 105°	19	2.4 ± 1.6	3.1 ± 1.5	na	c	‡
	240°, 120°	19	2.6 ± 1.5	2.9 ± 1.7	na	c	‡
	225°, 135°	17	2.7 ± 1.7	3.6 ± 2.1	na	c	‡

*Values from the repeated measures ANOVA; other values are from paired *t* tests. Levels of position with the same lowercase letter are not significantly different from one another (post-hoc pairwise contrasts).
‡Described in the text.
N = Number of hooves from which measurements were obtained. na = Not available.

dent where the medial value was less than the lateral value for dorsal angle combinations but the lateral value was greater than the medial value for palmar angle combinations ($P = 0.05$).

Discussion

The solar surface of the hoof capsule is intimately related to the transfer of ground reaction forces, and mediolateral symmetry has been a topic of discussion in hoof care for many years. Physical attributes of the hoof, including mediolateral symmetry, are possible indicators of risk for injury and unsoundness.[10,17] In 1 study[10] of hooves from Thoroughbred racehorse cadavers, horses that died or were euthanatized because of a nonmusculoskeletal disorder (control horses) had hooves with mediolateral asymmetry in hoof width greater than those of horses who sustained a catastrophic musculoskeletal injury. In general, control horses had hooves that were steeper on the medial side of the hoof wall and had larger mediolateral distances and sole area on the lateral side of the hoof than on the medial side of the hoof. Specifically for control horses, mean lateral wall angle was 95% of mean medial wall angle, mean medial ground surface width was 93% of mean lateral ground surface width, and mean medial sole width and sole area were 95% of respective mean lateral sole width and sole area. Horses with a catastrophic musculoskeletal injury or a suspensory apparatus failure had smaller differences (by 2.2 and 2.3°, respectively) between lateral and medial wall angles than control horses, smaller differences (by 2.5 and 3.1 mm, respectively) between lateral and medial ground surface widths, smaller differences (by 2.0 and 1.6 mm, respectively) between lateral and medial sole widths, and smaller differences (by 174 and 162 mm^2, respectively) between lateral and medial sole areas. Even smaller differences between lateral and medial sole widths and areas were observed in hooves of horses with a third metacarpal lateral condylar fracture. Although it is unknown whether there are cause and effect, adaptive, or indirect relationships between hoof conformation and musculoskeletal injuries, knowledge of the physical attributes of the hoof, including mediolateral asymmetry, is likely important for enhancing understanding of the etiopathogenesis of, and adaptation to, injuries. Because quantitative data regarding the solar surface of the hoof are scarce, and few methods for describing the surface are clear enough to allow accurate comparisons between results of research studies, the study reported here was intended to define a 3-D coordinate system and test the reproducibility of axis placement for this system. By means of this coordinate system, parameters for describing the solar surface of the hoof were defined and then used to characterize the solar surface of a sample of Thoroughbred racehorse hooves. Our data indicated that the coordinate system was reproducible, hoof width and radii had mediolateral differences in the ground surface plane, and almost all locations and parameters examined varied from dorsal to palmar in the ground surface plane and depth, but few of these variables had mediolateral differences.

The coordinate system was based on anatomical features in an attempt to increase the reproducibility of axis placement. The x-axis of the 3-D coordinate system was defined relative to the collateral sulci for 2 reasons. The depths of the collateral sulci separate the firm sole and underlying third phalanx from the softer frog and underlying digital cushion such that identification of these landmarks is straightforward and functionally meaningful. Moreover, their position in the ground surface plane is least likely to be altered by external influences (eg, hoof trimming) thus increasing consistency in axis placement. Because there were no significant differences between the medial and lateral locations of the deep collateral sulci, and because a post-hoc analysis of the overall mediolateral side power for a clinically important mean difference of 1 mm was 0.86, it is likely that the x-axis bisected the angle formed by the medial and lateral deep collateral sulci. Therefore, the method to establish the x-axis resulted in accurate placement. Additionally, the small differences between the experimental and standard axis and origin locations gathered from the reproducibility study indicated that this coordinate system was reproducible among investigators. Interobserver variation for individual measurements was not assessed. The use of multiple observers could be expected to increase the variability. Thus in the interests of limiting the variability, 1 observer was used in the study reported here.

The distance along the x-axis of the dorsal and palmar ground surface contact points of the hoof wall (the toe and heels of the wall) were used to derive the origin. Although hooves with abnormalities of the hoof wall were not evaluated in our study, the position of the origin would be affected by common alterations in the hoof wall including those associated with trimming, shoeing, abnormal wear, and hoof disorders. An alternative location for an origin could be the junction of the medial and lateral collateral sulci adjacent to the apex of the frog. For reasons similar to those supporting the definition of the x-axis of the 3-D coordinate system relative to the collateral sulci, this location would also be suitable as an origin, because it would likely be least alterable and readily apparent (at the junction of the harder and softer structures of the hoof capsule).

The x-y plane and the z-axis were based on the biomechanically relevant interface between a rigid ground surface and the hoof wall. The location and orientation of this plane relative to the position and axis of the limb would also be altered by wear, trimming, shoeing, and hoof disorders; however, this plane always remains the interface between the hoof and a rigid ground surface.

Our data, collected by means of the 3-D coordinate system from the left front hoof of Thoroughbred racehorses (euthanatized for any reason) were consistent with those of another study[10] involving Thoroughbred racehorse hooves obtained post mortem. In the study reported here, mean ground surface length and total foot length were each 97% of corresponding mean values reported previously. Similarly, our mean widest hoof width was 98% of that reported previously. These differences could stem from variations in axis placement and measurement location, as well as sample size and variation.

Mediolateral location and parameter differences in the ground surface plane were observed in more peripheral structures (eg, hoof wall), in which lateral distances were greater than medial distances. These findings were also consistent with those of the study[10] involving Thoroughbred racehorse hooves obtained post mortem. In our study, the lateral hoof width was 3% greater than medial hoof width, compared with a proportion of 7% in the same direction in the other study. Compared with data from the other study, medial and lateral hoof widths obtained in our study were 113 and 108% of reported values, respectively. However, in the other study, the sum of the medial and lateral mean hoof width values measured from 1 view is less than the mean widest hoof width measured from a different view; this suggests that the reported medial and lateral hoof widths may have been underestimated. Numerical discrepancies between studies could also be attributed either to differences in the axes system or differences between measurement techniques. In the study reported here, measurements were obtained directly from hoof specimens; measurements in the other study were obtained from video images via computer software. Although the lateral aspect of the hoof perimeter appeared to be wider than the medial aspect, the biomechanics and consequences of this are unclear.

Shaping of the hoof as a result of hoof care and hoof disease could have introduced variability in some of the locations and parameters. For example, the distal frog line, central sulcus edges, depth of the sole, the frog, and the ground contact surface of the wall are often altered by farriers. Size and shape of the landmarks vary with time from the last trimming or shoeing. Additionally, diseases of the hoof that can increase depth of the collateral sulci and central sulcus (eg, such as thrush) affect morphometric measurements. Nevertheless, hoof treatment and disease are inherent to the horse population. Accordingly, a meaningful analysis should be based on a sample of hooves that reflects these factors. The sample tested in the study of this report satisfied this criterion.

To verify that, for most variables, the sample size was great enough to avoid a type II statistical error notwithstanding the variability introduced by all sources including those mentioned, a post-hoc power analysis was completed for a clinically detectable and important mean difference for the mediolateral side comparison. In a study by Kane et al,[10] the mediolateral difference for 2 variables in the ground surface plane was calculated, and the resulting difference between these differences for the control sample and the sample associated with catastrophic musculoskeletal injury was 2 and 2.5 mm, respectively. Thus, a difference of 1 mm was chosen for the power analysis, because this difference could be detected clinically and conservatively represented functional importance (ie, approximately half the difference of 2 mm, which had been shown to be important functionally). With the actual sample size for each particular analysis, the power to detect a 1-mm difference between the lateral and medial mean values was > 0.75 for all variables except hoof wall radius (0.26), hoof wall thickness (0.46), and bar length (0.52). Accordingly, it was unlikely that the null hypothesis was falsely accepted for mediolateral comparisons. Similarly, mediolateral depth differences were not consistently observed among depth parameters that were measured on opposite sides of the dorsopalmar axis. Only dorsal aspects of the central sulcus and collateral sulci edges were significantly deeper medially than they were laterally, and the palmar aspect of the perimeter of the sole was deeper laterally than it was medially.

As noted for the mediolateral location and parameters in the ground surface plane, the measurement of depths was also affected by sources of variability. One source of variability in the depth measurements was associated with tissue compliance and hydration. Depth measurements likely varied with different levels of manual pressure that were applied during use of the measurement calipers.[3] Such pressure differences would be most noticeable in tissues of high compliance and high hydration (eg, the frog). This source of variation might be minimized if a mechanism to maintain an even measurement pressure could be incorporated into the calipers. Alternatively, a cast of the hoof would provide a rigid surface for measurements. A laser-based system, similar to that designed by Haut et al[18] to measure the surface of viscoelastic cartilage of diarthrodial joints, could be used without contacting the surface of the foot, thereby eliminating the deformation problem.

Despite the variability introduced in the depth measurements, the post-hoc power analysis revealed that powers for a clinically detectable level of difference of 1 mm were high ($P \geq 0.82$). Therefore, it is unlikely that differences would be detected from a clinical perspective.

A relationship between mediolateral imbalances in the ground surface plane with mediolateral imbalances in depths was not apparent. Only 1 (ie, sole at the perimeter) of the 12 locations that had a significant mediolateral imbalance in either the ground surface plane or in depth had significant asymmetry in both the ground surface plane and in depth. This may be associated with the general lack of mediolateral asymmetry in the depth parameters.

Dorsopalmar differences were generally consistent with the shape of the structures (eg, the palmarly located base of the frog being wider than the dorsally located apex). Some differences could be related to function. For example, the hoof wall was thickest from the toe through the quarters, which is an area of high wear in the unshod hoof; from the quarters toward the angles of the wall, at which the hoof spreads abaxially upon impact, the wall was comparatively thin[19,20] but increased in thickness at the angles. The radius of the hoof wall increased palmarly, possibly because the additional area assists in force distribution across the more compliant tissues of the frog and digital pads. However, hoof wall radii measurements would be affected by selection of the landmarks for the origin of the coordinate system. From morphologic data alone, other possible links between form and function are more speculative.

The data obtained in the study reported here are most applicable to Thoroughbred racehorses that died or were euthanatized during active training and racing. Hoof shape might be an indicator of either present or impending hoof injury or disease, an adaptation to injury, or an indicator for another factor that is related either to the etiopathogenesis of injury or adaptation to injury. For example, there is evidence that long-toe under-run heel hoof conformation is associated with musculoskeletal injuries in Thoroughbred racehorses.[10,21] If long-toe under-run heel hoof conformation is coincident with lack of mediolateral hoof asymmetry, either condition could be related to injury or another unknown factor that has a true causal relationship to injury or adaptation to injury. Additional information is needed before cause and effect relationships between hoof conformation, injury, and adaptations to injury and exercise can be established. Regardless, the standard measurement system allows comparison between hooves of normal horses and those of horses with hoof and leg problems. Knowledge of hoof shape may also assist in the development of simulations of hoof-surface interactions.

---

[a]PROC GLM, SAS Institute Inc, Cary, NC.

References

1. Stashak TS. The relationship between conformation and lameness. In: Stashak TS, ed. *Adams' lameness in horses*. Philadelphia: Lea & Febiger, 1987;72–95.

2. Balch O, White K, Butler D. Factors involved in the balancing of equine hooves. *J Am Vet Med Assoc* 1991;198:1980–1989.

3. Bertram JE, Gosline JM. Functional design of horse hoof keratin: the modulation of mechanical properties through hydration effects. *J Exp Biol* 1987;130:121–136.

4. Leach DH, Zoerb GC. Mechanical properties of equine hoof wall tissue. *Am J Vet Res* 1983;44:2190–2194.

5. Wagner IP, Hood DM, Hogan HA. Comparison of bending modulus and yield strength between outer stratum medium and stratum medium zona alba in equine hooves. *Am J Vet Res* 2001; 62:745–751.

6. Hood DM, Burt NW, Baker SJ, et al. Effects of ground surface on solar load distribution, in *Proceedings*. 43rd Annu Meet Am Assoc Equine Pract 1997;360–362.

7. Hood DM, Taylor D, Wagner IP. Effects of ground surface deformability, trimming, and shoeing on quasistatic hoof loading patterns in horses. *Am J Vet Res* 2001;62:895–900.

8. Douglas JE, Mittal C, Thomason JJ, et al. The modulus of elasticity of equine hoof wall: implications for the mechanical function of the hoof. *J Exp Biol* 1996;199:1829–1836.

9. Ratzlaff MH, Hyde ML, Grant BD, et al. Measurement of vertical forces and temporal components of the strides of horses using instrumented shoes. *Equine Vet Sci* 1990;10:23–35.

10. Kane AJ, Stover SM, Gardner IA, et al. Hoof size, shape, and balance as possible risk factors for catastrophic musculoskeletal injury of Thoroughbred racehorses. *Am J Vet Res* 1998;59:1545–1552.

11. Sparks J. New horseshoe approximates the unshod equine foot. *Vet Med Small Anim Clin* 1971;66:110–111.

12. Kane AJ, Stover SM, Gardner IA, et al. Horseshoe characteristics as possible risk factors for fatal musculoskeletal injury of thoroughbred racehorses. *Am J Vet Res* 1996;57:1147–1152.

13. Barrey E. Investigation of the vertical hoof force distribution in the equine forelimb with an instrumented horseboot. *Equine Vet J Suppl* 1990;June:35–38.

14. Caudron I, Grulke S, Farnir F, et al. In-shoe foot force sensor to assess hoof balance determined by radiographic method in ponies trotting on a treadmill. *Vet Q* 1998;20:131–135.

15. Colahan P, Leach D, Muir G. Center of pressure location of the hoof with and without hoof wedges. *Equine Exerc Physiol* 1991;3:113–119.

16. Wilson AM, Seelig TJ, Shield RA, et al. The effect of foot imbalance on point of force application in the horse. *Equine Vet J* 1998;30:540–545.

17. Ruohoniemi M, Raekallio M, Tulamo R, et al. Relationship between ossification of the cartilages of the foot and conformation and radiographic measurements of the front feet in Finnhorses. *Equine Vet J* 1997;29:44–48.

18. Haut TL, Hull ML. A high-accuracy three-dimensional coordinate digitizing system for reconstructing the geometry of diarthrodial joints. *J Biomech* 1998;31:571–577.

19. Thomason JJ. Variation in surface strain on the equine hoof wall at the midstep with shoeing, gait, substrate, direction of travel, and hoof shape. *Equine Vet J Suppl* 1998;26:86–95.

20. Newlyn HA, Collins SN, Cope BC, et al. Finite element analysis of static loading in donkey hoof wall. *Equine Vet J Suppl* 1998;26:103–110.

21. Balch OK, Helman RG, Collier MA. Underrun heels and toe-grab length as possible risk factors for catastrophic musculoskeletal injuries in Oklahoma racehorses, in *Proceedings*. 47th Annu Meet Am Assoc Equine Pract 2001;334–338.